Available online at www.sciencedirect.com
SCIENCE DIRECT®
PERGAMON
International Journal of Heat and Mass Transfer 46 (2003) 3441–3450
International Journal of HEAT and MASS TRANSFER
www.elsevier.com/locate/ijhmt

Entropy generation at the onset of natural convection

M. Magherbi [a], H. Abbassi [b], A. Ben Brahim [a,*]

[a] Engineers National School of Gabes, Omar Ibn El Khattab Street, 6029 Gabes, Tunisia
[b] Sciences Faculty of Sfax, BP 763, 3038, Tunisia

Received 5 April 2002; received in revised form 27 January 2003

Abstract

The entropy generation due to heat transfer and friction has been determined in transient state for laminar natural convection by solving numerically the mass, momentum and energy balance equations, using a control volume finite-element method. The variations of the total entropy generation as function of time for Rayleigh number and irreversibility distribution ratio set at $10^3 \leqslant Ra \leqslant 10^5$ and $10^{-4} \leqslant \varphi \leqslant 10^{-1}$ were investigated. The evolution of the maximum of entropy generation with the Rayleigh number is studied. The effect of the irreversibility distribution ratio on the maximum entropy generation and the entropy generation in steady state are analyzed. The irreversibility maps for Rayleigh number set at $10^3 \leqslant Ra \leqslant 10^5$ and irreversibility distribution ratio $\varphi = 10^{-4}$ are plotted.

Keywords: Entropy; Generation; Steady; Unsteady; Cavity

1. Introduction

Thermodynamic system submitted to thermal gradient, friction effects, diffusion, chemical reaction..., are subject to energy losses, which induces entropy generation in the system. The optimal design criteria for thermodynamic systems can be achieved by analyzing entropy generation in the systems. Entropy generation has recently been the topic of great interest in fields such as heat exchangers, turbomachinery, electronic cooling, porous media and combustion. Many studies have been published on entropy generation. Datta [1] investigated the entropy generation in a confined laminar diffusion flame. It has been proved that the major contribution to the entropy generation is due to heat transfer within the flame. Baytas [2,3] presented a numerical study on the minimization of entropy generation in an inclined enclosure [2] and inclined porous cavity [3]. The influence of Rayleigh number, Bejan number and inclination angle, on entropy generation, are evaluated. It has been established that minimum entropy generation considerably depends on the inclination angle of the enclosure. Bejan [4] showed that the entropy generation for forced convective heat transfer is due to temperature gradient and viscous effect in the fluid. Demirel and Kahraman [5] studied the entropy generation in a rectangular packed duct with wall heat flux. It was found that the irreversibility distribution is not continuous through the wall and core regions. Sahim [6] analytically investigated entropy generation in turbulent liquid flow through a smooth duct subjected to constant wall temperature. It was found that constant viscosity assumption may yield a considerable amount of deviation on entropy generation. Entropy generation and Lyapunov instability at the onset of turbulent convection were examined by Castillo and Hoover [7]. They showed that the two flow morphologies at the same Rayleigh number have different rates of entropy generation and different Lyapunov exponent. The harmonic flow produces entropy at greater rate whereas the chaotic flow has a larger maximum Lyapunov exponent. Different research on local entropy generation in heat exchangers are available in the literature [8,9].

The numerical study about entropy generation in transient state for natural convection has not yet been encountered. The present paper reports a numerical

* Corresponding author. Tel.: +216-753-92100; fax: +216-753-92190.
E-mail address: ammar.benbrahim@enig.rnu.tn (A. Ben Brahim).

0017-9310/03/$ - see front matter
doi:10.1016/S0017-9310(03)00133-9

Nomenclature

a	thermal diffusivity ($m^2\,s^{-1}$)
Be	Bejan number
g	acceleration due to gravity ($m\,s^{-2}$)
k	conductivity ($J\,m^{-1}\,s^{-1}\,K^{-1}$)
L	cavity length (m)
p	pressure ($N\,m^{-2}$)
P	dimensionless pressure
Pr	Prandtl number
Ra	Rayleigh number
$\dot{S}$	entropy generation per unit volume ($J\,m^{-3}\,s^{-1}\,K^{-1}$)
t	time (s)
T	temperature (K)
T_0	bulk temperature (K), $T_0 = (T_h + T_c)/2$ (K)
ΔT	temperature difference, $\Delta T = T_h - T_c$ (K)
ϑ	system volume
$\vec{v}$	velocity vector
$\vec{V}$	dimensionless velocity vector
u, v	velocity components in x, y directions ($m\,s^{-1}$)
U, V	dimensionless velocity, components in x, y directions
x, y	cartesian coordinates (m)
X, Y	dimensionless Cartesian coordinates

Greek symbols

β	coefficient of thermal expansion, (K^{-1})
θ	dimensionless temperature
μ	dynamic viscosity, ($kg\,m^{-1}\,s^{-1}$)
ν	cinematic viscosity, ($m^2\,s^{-1}$)
φ	irreversibility distribution ratio
τ	shear tensor, ($N\,m^{-2}$)
ζ	dimensionless time

Subscripts

a	dimensionless
c	cold
f	friction effect
h	heat transfer/hot
l	local
p	steady state
T	total

study of entropy generation in transient state in a vertical cavity submitted to an horizontal thermal gradient. The evolution of entropy generation, and the Bejan number in transient state for laminar natural convection were studied . The effects of the Rayleigh number and the irreversibility distribution ratio on the entropy generation were examined. The local irreversibility maps in steady state as function of Rayleigh number were given.

2. Mathematical modeling

2.1. Flow and governing equations

Consider the flow of a Newtonian Boussinesq incompressible fluid enclosed in a differential heated cavity as shown in Fig. 1. The set of dimensionless governing equations in transient state are:

$$\frac{\partial U}{\partial X} + \frac{\partial V}{\partial Y} = 0 \tag{1}$$

$$\frac{\partial U}{\partial \zeta} + \mathrm{div}\vec{J}_U = -\frac{\partial P}{\partial X} \tag{2}$$

$$\frac{\partial V}{\partial \zeta} + \mathrm{div}\vec{J}_V = -\frac{\partial P}{\partial Y} + Ra \cdot Pr \cdot \theta \tag{3}$$

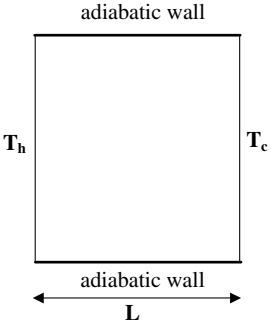

Fig. 1. Schematic view of 2D cavity.

$$\frac{\partial \theta}{\partial \zeta} + \mathrm{div}\vec{J}_\theta = 0 \tag{4}$$

with

$$\vec{J}_U = U\vec{V} - Pr \cdot \overrightarrow{\mathrm{grad}}U \tag{5}$$

$$\vec{J}_V = V\vec{V} - Pr \cdot \overrightarrow{\mathrm{grad}}V \tag{6}$$

$$\vec{J}_\theta = \theta\vec{V} - \overrightarrow{\mathrm{grad}}\theta \tag{7}$$

where the dimensionless variables are defined by:

$$X=\frac{x}{L};\quad Y=\frac{y}{L};\quad U=\frac{uL}{a};\quad V=\frac{vL}{a};$$
$$\theta=\frac{T-T_0}{T_h-T_c};\quad P=\frac{pL^2}{\rho a^2};\quad Ra=\frac{\beta g\Delta T L^3}{va};$$
$$\zeta=\frac{at}{L^2};\quad Pr=\frac{v}{a} \tag{8}$$

2.2. Boundary and initial conditions

The boundary conditions appropriate to laminar flow within the differential heated cavity are:

$U=V=0$ for all walls

$\theta=0.5$ on plane $X=0$

$\theta=-0.5$ on plane $X=1$

$\dfrac{\partial\theta}{\partial Y}=0$ on planes $Y=1$ and $Y=0$

The initial conditions are:

$\zeta=0$

$U=V=0, P=0$ and $\theta=0.5-X$ for whole space

2.3. Entropy generation

The existence of a thermal gradient between the vertical walls of the enclosure sets the fluid in a non-equilibrium state which causes entropy generation in the system. According to local thermodynamic equilibrium with linear transport theory, the local entropy generation is given by [2,3]:

$$\dot{S}_l=\frac{k}{T_0^2}(\vec{\nabla}T)^2+\frac{\bar{\bar{\tau}}:\bar{\bar{\nabla}}\vec{v}}{T_0} \tag{9}$$

In the case of two dimensional Cartesian system Eq. (9) can be written as:

$$\dot{S}_l=\frac{k}{T_0^2}\left[\left(\frac{\partial T}{\partial x}\right)^2+\left(\frac{\partial T}{\partial y}\right)^2\right]+\frac{\mu}{T_0}\left[2\left(\frac{\partial u}{\partial x}\right)^2+2\left(\frac{\partial v}{\partial x}\right)^2+\left(\frac{\partial u}{\partial y}+\frac{\partial v}{\partial x}\right)^2\right] \tag{10}$$

The local entropy generation can be made dimensionless by using the dimensionless variables listed in Eq. (8):

$$\dot{S}_{l,a}=\dot{S}_{l,a,h}+\dot{S}_{l,a,f} \tag{11}$$

where:

$$\dot{S}_{l,a,h}=\left[\left(\frac{\partial\theta}{\partial X}\right)^2+\left(\frac{\partial\theta}{\partial Y}\right)^2\right] \tag{12}$$

$$\dot{S}_{l,a,f}=\varphi\left[2\left(\frac{\partial U}{\partial X}\right)^2+2\left(\frac{\partial V}{\partial Y}\right)^2+\left(\frac{\partial U}{\partial Y}+\frac{\partial V}{\partial X}\right)^2\right] \tag{13}$$

$$\varphi=\frac{\mu T_0}{k}\left(\frac{a}{L(\Delta T)}\right)^2 \tag{14}$$

The first term on the right-hand side of Eq. (11) shows the local entropy generation due to heat transfer ($\dot{S}_{l,a,h}$), while the second term shows the local entropy generation due to fluid friction ($\dot{S}_{l,a,f}$). The dimensionless total entropy generation is the integral over the system volume of the dimensionless local entropy generation:

$$\dot{S}_{T,a}=\int_{\vartheta}\dot{S}_{l,a}\,d\vartheta \tag{15}$$

An alternative irreversibility distribution parameter called Bejan number (Be) [5] is given in dimensionless form as follows:

$$Be=\frac{\dot{S}_{l,a,h}}{\dot{S}_{l,a}} \tag{16}$$

When $Be\gg 1/2$, the irreversibility due to heat transfer dominates. For $Be\ll 1/2$ the irreversibility due to viscous effect dominates. For $Be=1/2$ heat transfer and fluid friction entropy generation are equal. From the known temperature and velocity fields at time ζ given by solving Eqs. (1)–(4), the dimensionless local entropy generation can be evaluated in each point of the domain by Eq. (11). Using Eq. (15) the dimensionless total entropy generation can be obtained. By varying ζ from 0 to steady state, the transient evolution of dimensionless total entropy generation and the Bejan number can be determined.

3. Numerical procedure

A modified version of the control volume finite-element method (CVFEM) of Saabas and Baliga [10] is adapted to the standard staggered grid in which pressure and velocity components are stored at different points. The SIMPLER algorithm was applied to resolve the pressure–velocity coupling in conjunction with an alternating direction implicit (ADI) scheme for performing the time evolution. A shape function describing the variation of the dependant variable ϕ ($=U, V$ or θ) is needed to calculate the flux across the control-volume faces. We have followed Saabas and Baliga [10] in assuming linear and exponential variations respectively when the dependant variable ϕ is calculated in the diffusive and in the convective terms of the conservation equations. More details and discussions about CVFEM are available in the works of Prakash [11], Hookey [12], Elkaim et al. [13], Saabas and Baliga [10] and in many

other works. The numerical code used here is described and validated in details in Abbassi et al. [14].

4. Results and discussions

In this investigation, the Prandtl number was fixed at 0.7. The Rayleigh number and the irreversibility distribution ratio are in the ranges of $10^3 \leqslant Ra \leqslant 10^5$ and $10^{-4} \leqslant \varphi \leqslant 10^{-1}$. Figs. 2–4 illustrate the variations of the dimensionless total entropy generation in the transient state for different irreversibility distribution ratios φ. It can be concluded that the dimensionless total entropy

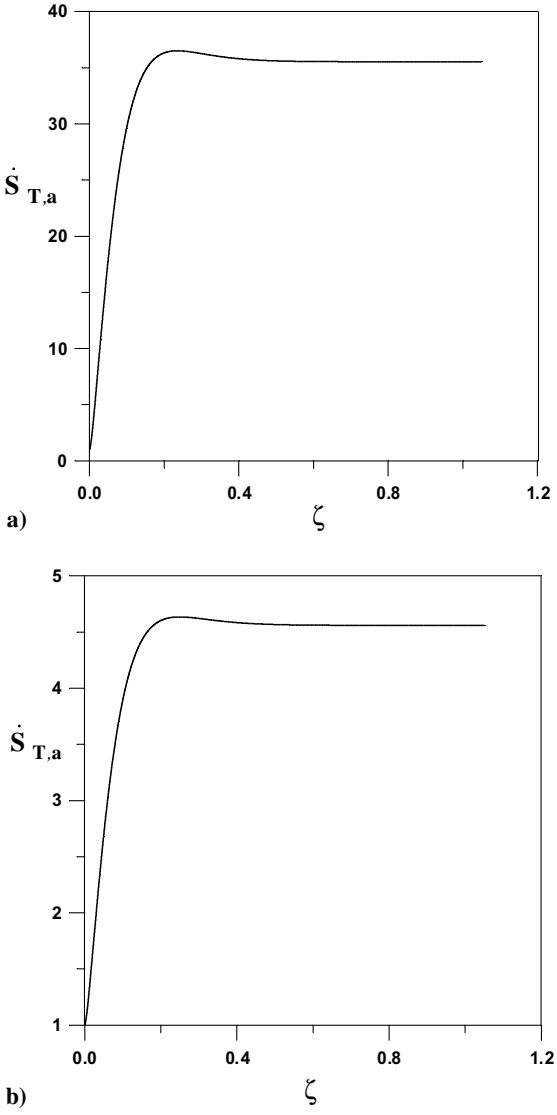

Fig. 2. Dimensionless total entropy generation versus time for $Ra = 10^3$: (a) $\varphi = 10^{-1}$, (b) $\varphi = 10^{-2}$.

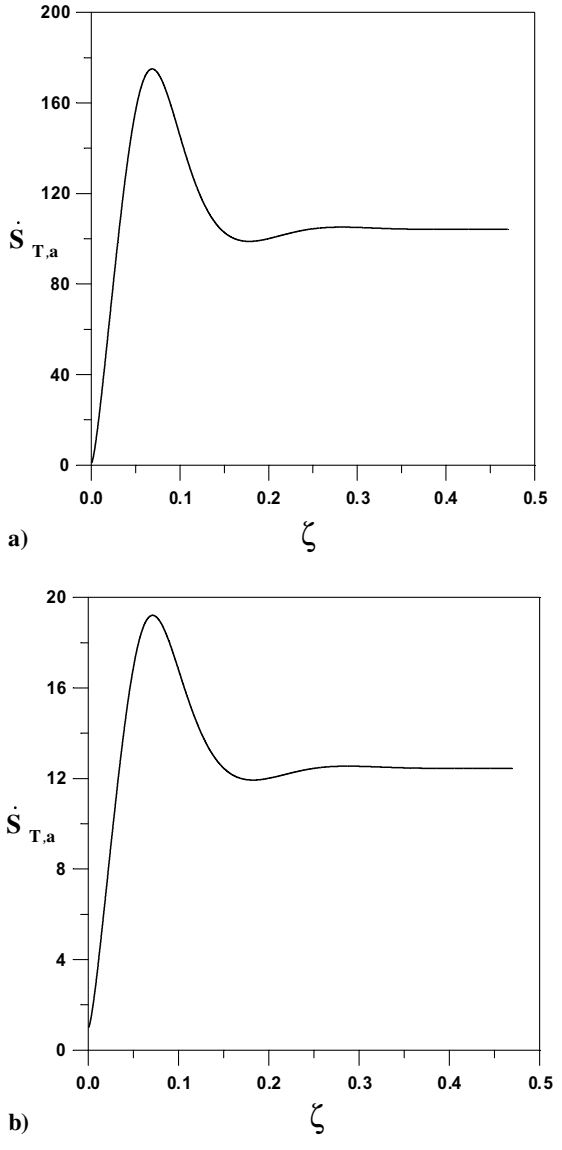

Fig. 3. Dimensionless total entropy generation versus time for $Ra = 10^4$: (a) $\varphi = 10^{-2}$, (b) $\varphi = 10^{-3}$.

generation $\dot{S}_{T,a}$ has a maximum Max($\dot{S}_{T,a}$) at the onset of the transient state, then decreases to reach a constant value in the steady state. This maximum is reached as faster as the Rayleigh number is important. It can be seen from Fig. 2 that for small Rayleigh numbers, the total entropy generation tends towards a constant value asymptotically, whereas for relatively important Rayleigh numbers, precisely greater then a critical Rayleigh number $Ra_c = 5200$, an oscillation of the entropy generation can be observed before reaching the steady state, Figs. 3 and 4. As seen in Figs. 3 and 4, the amplitude and the number of oscillations of the entropy generation are

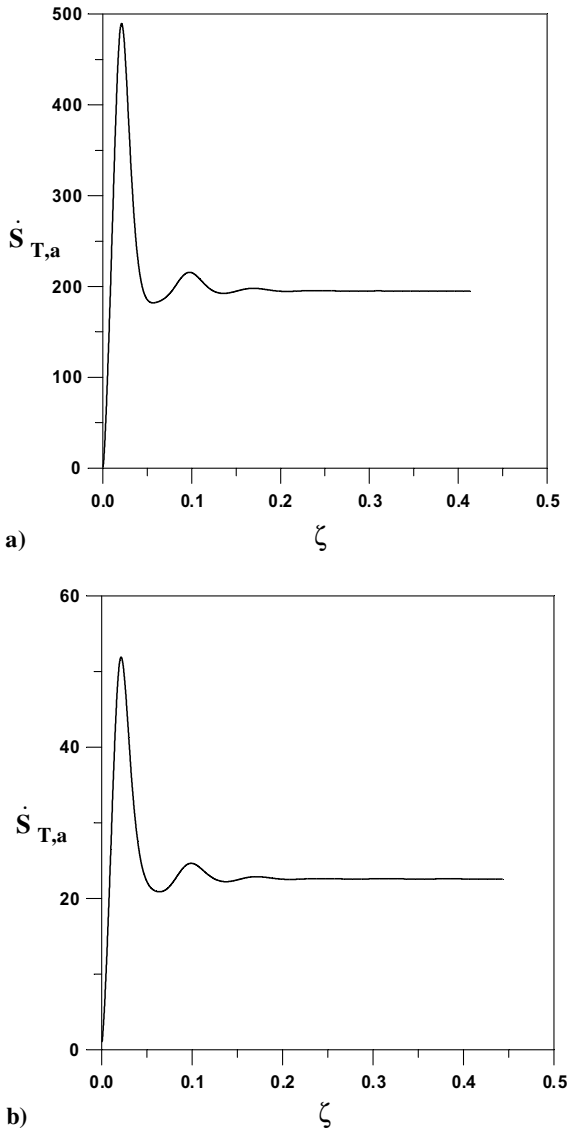

Fig. 4. Dimensionless total entropy generation versus time for $Ra = 10^5$: (a) $\varphi = 10^{-3}$, (b) $\varphi = 10^{-4}$.

as important as the Rayleigh number increases. Fluctuations of the total entropy generation at high Rayleigh numbers indicate that the flow exhibits oscillatory behavior which depends on the boundary conditions. At the very beginning of the transient state heat transfer is mainly due to heat conduction. The isotherms are nearly parallel to the active walls generating an horizontal temperature gradient. The streamlines are those of a single spiral with its center being at the center of the cavity. As time proceeds the isotherms are gradually deformed by convection generating a vertical temperature gradient while the horizontal temperature gradient diminishes in the center of the cavity and becomes locally negative which causes an elongation of the central streamline and the development of a second spiral in the core, practically at the dimensionless time $\zeta = 5 \times 10^{-2}$, just before the entropy generation reaches its first minimum. This transition from a single to a double configuration may induce generation of internal waves in the velocity and temperature fields who can be at the origin of the oscillations of the whole cavity and consequently of the entropy generation. The current result is consistent with the findings of Ivey [15], Schladow [16] and Patterson and Armfield [17] who showed the existence of transient oscillations in enclosures consisting of two isothermal vertical walls and two adiabatic horizontal walls. Ivey [15] claimed the transient oscillations occurred because of an internal hydraulic jump with an increase of the horizontal intrusion layers. These oscillations were stated to disappear as the interior is set in motion and stratifies in temperature, increasing the thickness of the intrusion and flooding the hydraulic jump. Transient oscillations consisting of two distinct boundary layer instabilities and a whole cavity oscillations were observed by Schladow [16]. The whole cavity oscillations were attributed to the horizontal pressure gradient established by changes in the intrusion temperature field. Similar observations are given by Patterson and Armfield [17]. The two boundary layer oscillations were attributed to travelling wave instability on the boundary layer induced first by the leading edge effect of the vertical boundary layer and second by the impact of the horizontal intrusion from the opposing vertical wall with the boundary layer. The whole cavity oscillations are said to be caused by the splitting of the horizontal intrusion as it impacts the opposite wall. From a thermodynamics view point, the asymptotic behavior of the total entropy generation with time at small Rayleigh numbers shows that the system is in the linear branch of the thermodynamics of irreversible processes where the famous reciprocity relations of Onsager are applicable. In fact for small Rayleigh number the steady state is sufficiently close the equilibrium state, therefore the system returns directly towards the steady state and the Prigogine's theorem of minimum entropy production is verified. For higher Rayleigh numbers ($Ra > Ra_c$) the steady state is relatively far from the equilibrium state , then a rotation around the steady state is possible, and the system is in the case of a spiral approach towards this state corresponding to an oscillation of the total entropy generation. Consequently, the system evolves in the non-linear branch of irreversible phenomena. Since the thermal gradient gives birth to a convection regime, new coupling effects are introduced. These coupling effects are not considered by the reciprocity relations of Onsager due to the fact that convection is negligible for small Rayleigh numbers (linear branch) and the flow is dominated by conduction

only. The transition from the linear thermodynamics domain to the non-linear thermodynamics domain is made at a critical Rayleigh number $Ra_c = 5200$. As seen in Figs. 5–7 the initial value of the Bejan number (Be) is $Be = 1$. This is due to zero initial condition of velocity vector, which induces that the entropy generation due to viscous effects is zero and therefore the total entropy generation is reduced to the entropy generation due to heat transfer ($\dot{S}_{l,a} = \dot{S}_{l,a,h}$). Figs. 5–7 show that the Bejan number decreases (rapidly for higher Ra) at the very beginning of the transient state and reaches a minimum value at practically the same time that entropy generation reaches its maximum. This is caused by the onset of the convection regime, the flow in the hot and cold viscous layers accelerates (rapidly for higher Ra) at the onset of the transient state and the entropy generation due to fluid friction begins to play a significant role ($\dot{S}_{l,a,f} > 0$). As can be seen in Figs. 6 and 7 the transient oscillatory behavior of the Bejan number at higher Rayleigh numbers is due to the oscillations of the entropy generation. In the steady state Figs. 5–7 show that the domination of one of the two effects (thermal or viscous) on total entropy generation is highly depends on the Rayleigh number and the irreversibility distribution ratio. For a given value of the irreversibility distribution ratio, the Bejan number decreases with increasing Rayleigh number therefore viscous effects irreversibility becomes significant and begins to dominate heat transfer irreversibility. Graphs of the maximum of the total entropy generation $\mathrm{Max}(\dot{S}_{T,a})$ as function of Rayleigh number at different irreversibility distribution ratio φ are shown in Fig. 8. At low irreversibility distribution ratios (as low as $\varphi \leqslant 10^{-4}$) $\mathrm{Max}(\dot{S}_{T,a})$ takes on small values even at high Rayleigh numbers. However,

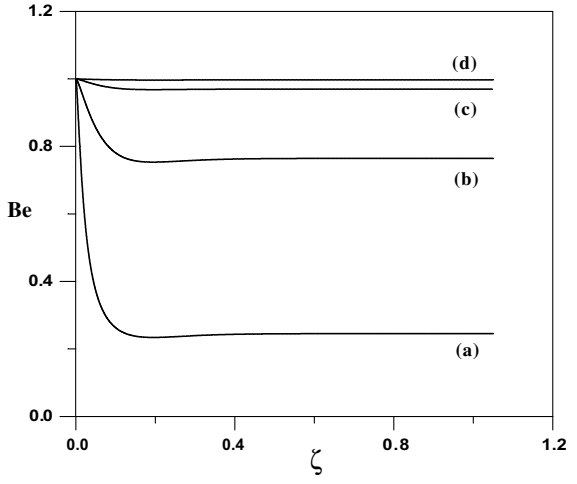

Fig. 5. Variation of Bejan number versus time for $Ra = 10^3$: (a) $\varphi = 10^{-2}$, (b) $\varphi = 10^{-3}$ and (c) $\varphi = 10^{-4}$, (d) $\varphi = 10^{-5}$.

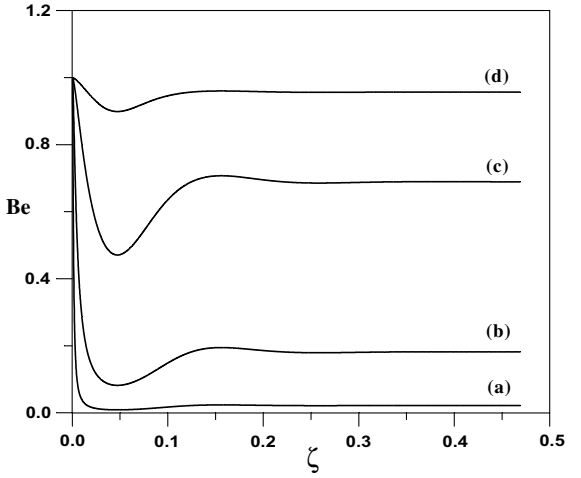

Fig. 6. Variation of Bejan number versus time for $Ra = 10^4$: (a) $\varphi = 10^{-2}$, (b) $\varphi = 10^{-3}$, (c) $\varphi = 10^{-4}$ and (d) $\varphi = 10^{-5}$.

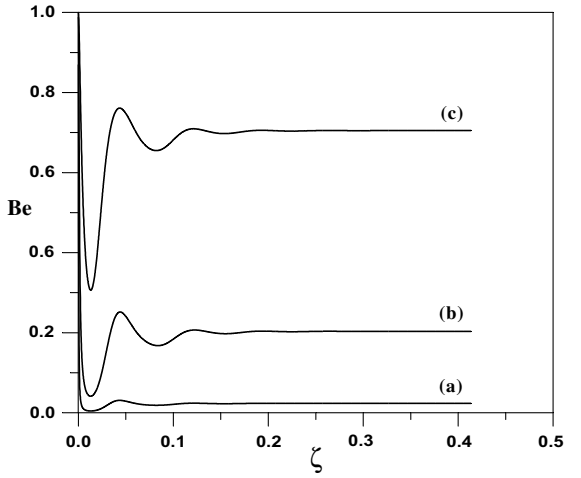

Fig. 7. Variation of Bejan number versus time for $Ra = 10^5$: (a) $\varphi = 10^{-3}$, (b) $\varphi = 10^{-4}$ and (c) $\varphi = 10^{-5}$.

for $\varphi \geqslant 10^{-3}$, $\mathrm{Max}(\dot{S}_{T,a})$ increases rapidly. Similar observations can be made about the evolution of the total entropy generation $\dot{S}_{T,a,p}$ as a function of the Rayleigh number during the steady state as seen in Fig. 9. At low value of Rayleigh numbers ($Ra = 10^3$), the difference between the maximum of the total entropy generation $\mathrm{Max}(\dot{S}_{T,a})$ and the entropy generation in steady state $\dot{S}_{T,a,p}$ (denoted the gap (G) in Fig. 10(a)), has low value. This is because the disruption introduced into the system is small during the transient state at low Rayleigh numbers. Fig. 10(b) and (c), show that the gap considerably increases with increasing Rayleigh number, at high Rayleigh numbers, the size of the gap (G) is large even for small irreversibility distribution ratios. It is

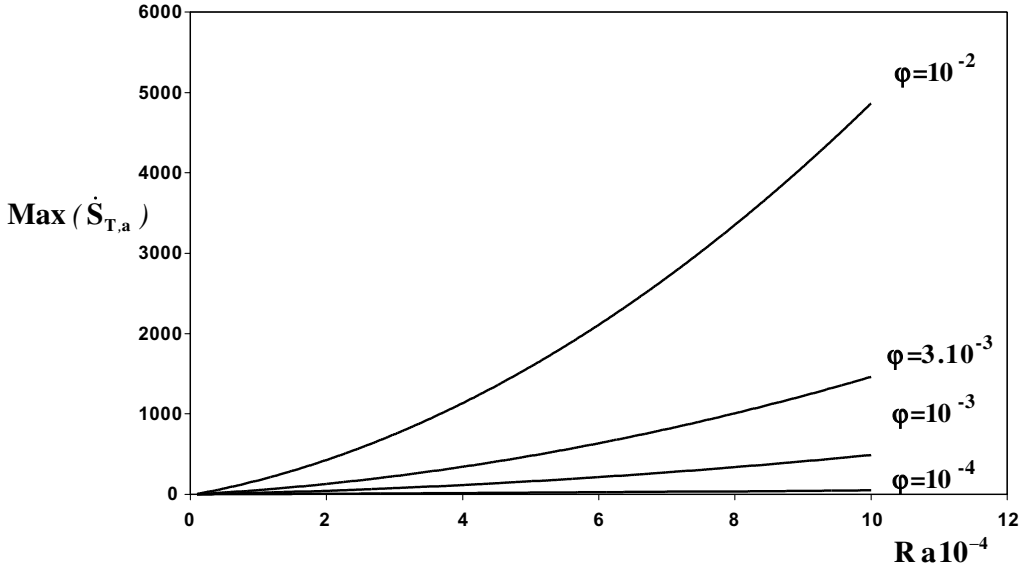

Fig. 8. Evolution of the maximum of the dimensionless total entropy generation versus Rayleigh number and distribution irreversibility ratio $\varphi = 10^{-4}$, 10^{-3}, 3.3×10^{-3}, and 10^{-2}.

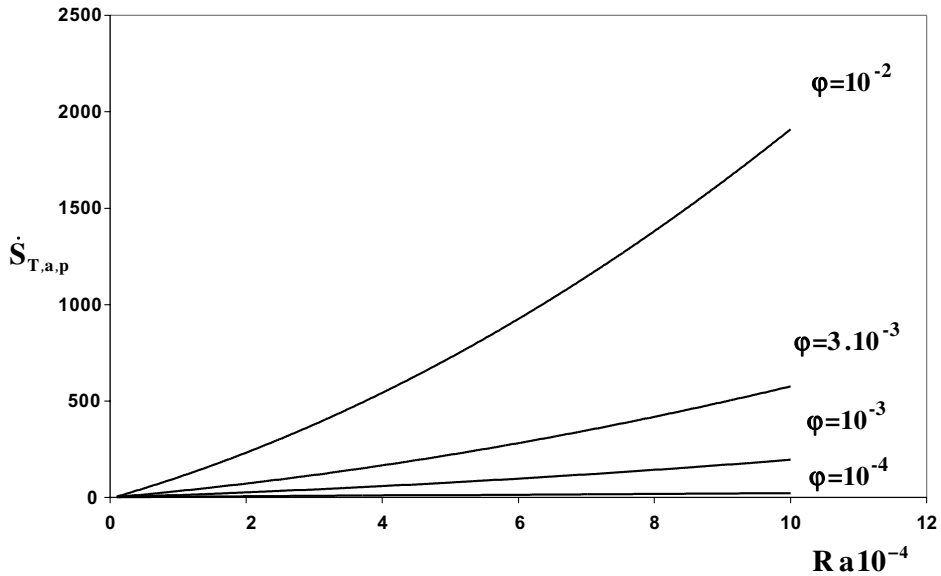

Fig. 9. Variation of the dimensionless total entropy generation in steady state versus Rayleigh number and distribution irreversibility ratio $\varphi = 10^{-4}$, 10^{-3}, 3.3×10^{-3}, and 10^{-2}.

important to note the linear behavior of the gap as function of the irreversibility distribution ratio φ for $Ra > Ra_c$. The local heat transfer irreversibility maps are shown in Fig. 11. As seen in Fig. 11(a), for $Ra = 10^3$ entropy generation covers the whole domain except the upper and lower corners for the heated and cooled walls, respectively. Fig. 11(b) and (c), show that as the Rayleigh number increases , the local entropy generation is increasingly confined to the neighborhood of the active walls of the enclosure. This is due to heat transfer irreversibility, because large heat transfer is confined to these locations. Fig. 12 show the local entropy generation maps due to heat transfer and fluid friction. It can be concluded that entropy generation covers the whole

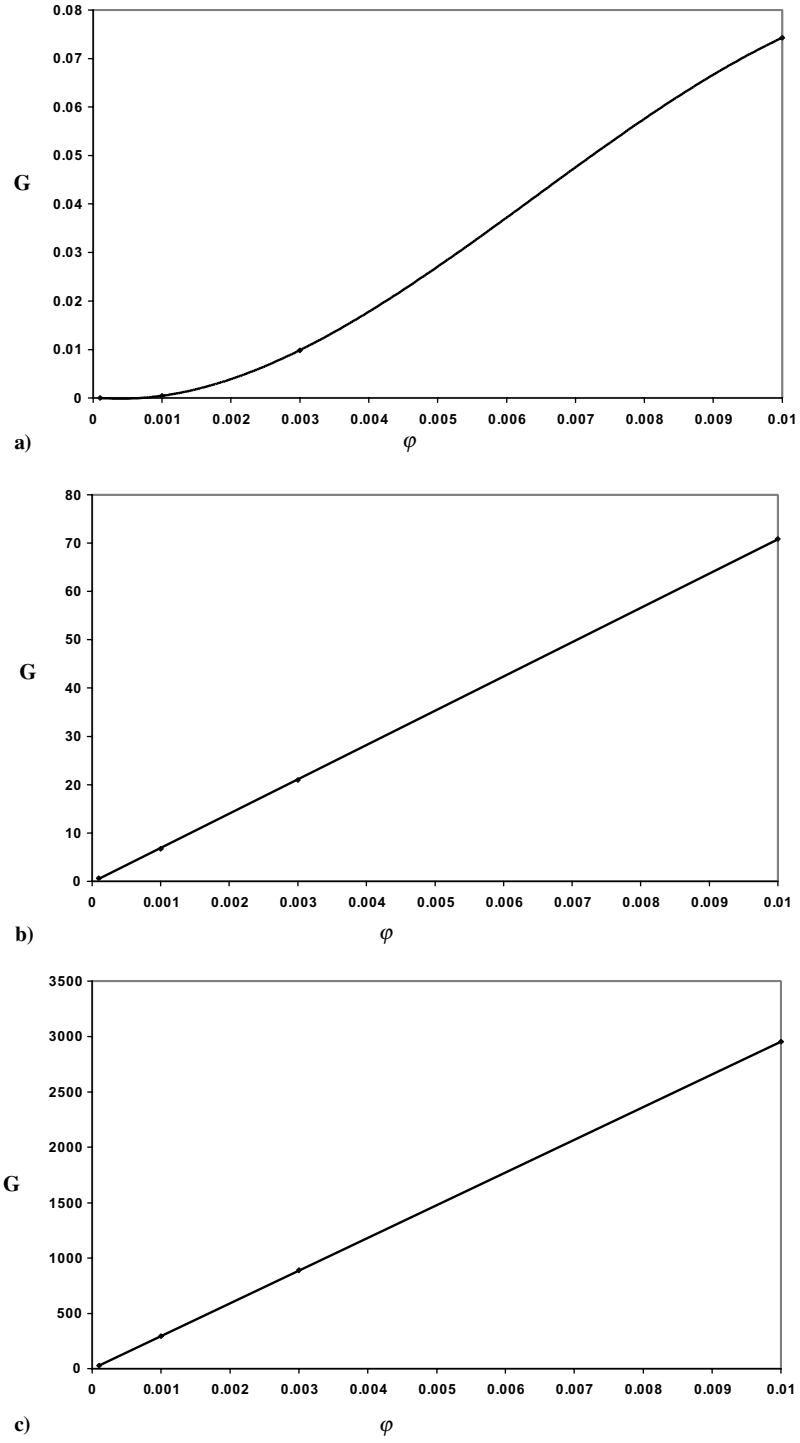

Fig. 10. Variation of the gap with irreversibility distribution ratio: (a) $Ra = 10^3$, (b) $Ra = 10^4$ and (c) $Ra = 10^5$.

domain for $Ra = 10^3$, Fig. 12(a). This covered domain reduces with increasing Rayleigh number, Fig. 12(b) and (c). For higher Rayleigh number, Fig. 12(c) shows that the entropy generation is localized along the walls only. This is due to the boundary layer regime at higher Rayleigh numbers.

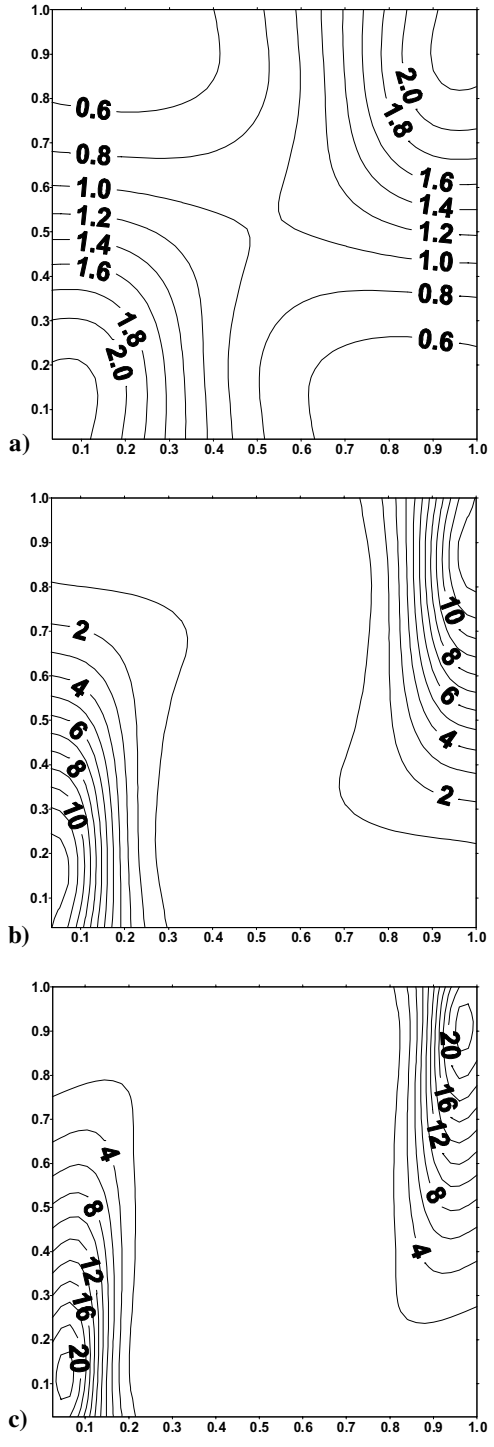

Fig. 11. Entropy generation maps due to heat transfer: (a) $Ra = 10^3$, (b) $Ra = 10^4$ and (c) $Ra = 10^5$.

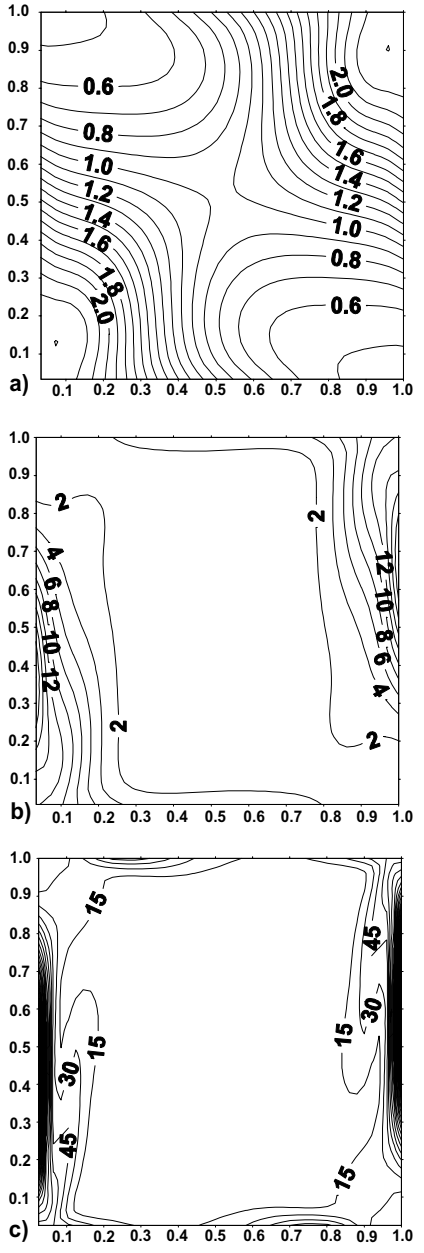

Fig. 12. Entropy generation maps due to heat transfer and fluid friction for irreversibility distribution ratio $\varphi = 10^{-4}$: (a) $Ra = 10^3$, (b) $Ra = 10^4$ and (c) $Ra = 10^5$.

5. Conclusion

Entropy generation in transient state for natural convection was calculated numerically by using a control volume finite-element method. The influence of the Rayleigh number and the irreversibility distribution ratio on the total entropy generation and the Bejan

number are evaluated. Results show that the total entropy generation has a maximum value at the onset of the transient state, which increases with the Rayleigh number and the irreversibility distribution ratio. It was found that entropy generation asymptotically tends towards a constant value at low Rayleigh numbers, whereas an oscillation of the entropy generation was observed for higher Rayleigh numbers, before reaching the steady state. Results show that the flow exhibits oscillatory behavior at high Rayleigh numbers. It was found that beyond a critical value of the Rayleigh number, the Prigogine's theorem of minimum entropy production is not verified and the system is out of the linear branch of irreversible phenomena. Results show that the Bejan number takes a minimum value in the beginning of the transient state which decreases with increasing Rayleigh number and irreversibility distribution ratio. Results show that for increasing Rayleigh number viscous effects irreversibility begins to dominate heat transfer irreversibility. In the steady state, entropy generation is spread over the whole domain at small Rayleigh numbers, but is confined to the neighborhood of the active walls at high Rayleigh numbers.

References

[1] A. Datta, Entropy generation in a confined laminar diffusion flame, Combust. Sci. Technol. 159 (2000) 39–56.
[2] A.C. Baytas, Optimization in an inclined enclosure for minimum entropy generation in natural convection, Int. J. Heat Mass Transfer 22 (1997) 145–155.
[3] A.C. Baytas, Entropy generation for natural convection in an inclined porous cavity, Int. J. Heat Mass Transfer 43 (2000) 2089–2099.
[4] A. Bejan, Convection Heat Transfer, second ed., Wiley, New York, 1995.
[5] Y. Demirel, R. Kahraman, Entropy generation in a rectangular packed duct with wall heat flux, Int. J. Heat Mass Transfer 42 (1999) 2337–2344.
[6] A.Z. Sahim, Entropy generation in a turbulent liquid flow through a smooth duct subjected to constant wall temperature, Int. J. Heat Mass Transfer 43 (2000) 1469–1478.
[7] V.M. Castello, W.G. Hoover, Entropy production and Lyapunov instability at the onset of turbulent convection, Phys. Rev. E 58 (1998) 7350–7354.
[8] A. Bejan, The concept of irreversibility in heat exchanger design counter flow heat exchangers for gas-to-gas applications, J. Heat Transfer 99 (1997) 334–380.
[9] M.K. Drost, M.D. White, Numerical prediction of local entropy generation in an impinging jet, J. Heat Transfer 113 (1991) 427–434.
[10] H.J. Saabas, B.R. Baliga, Co-located equal-order control-volume finite-element method for multidimensional, incompressible, fluid flow, Numer. Heat Transfer, part B 26 (1994) 381–407.
[11] C. Prakash, An improved control volume finite-element method for heat and mass transfer, and for fluid flow using equal order velocity–pressure interpolation, Numer. Heat Transfer 9 (1986) 253–276.
[12] N.A. Hookey, A CVFEM for two-dimensional viscous compressible fluid flow, PhD thesis, McGill University, Montreal, Quebec, 1989.
[13] D. Elkaim, M. Reggio, R. Camarero, Numerical solution of reactive laminar flow by a control-volume based finite-element method and the vorticity-stream function formulation, Numer. Heat Transfer, part B 20 (1991) 223–240.
[14] H. Abbassi, S. Turki, S. Ben Nasrallah, Mixed convection in a plane channel with a built-in triangular prism, Numer. Heat Transfer, Part A 39 (3) (2001) 307–320.
[15] G.N. Ivey, Experiments on transient natural convection in a cavity, J. Fluid Mech. 144 (1984) 389–401.
[16] S.G. Schladow, Oscillatory motion in aside-heated cavity, J. Fluid Mech. 213 (1990) 589–610.
[17] J.C. Patterson, S.W. Armfield, Transient features of natural convection in a cavity, J. Fluid Mech. 219 (1990) 469–497.